OPEN ACCESS

Optimization of plasma parameters for the production of silicon nano-crystals

New Journal of Physics
An Institute of Physics and Deutsche Physikalische Gesellschaft Journal

Optimization of plasma parameters for the production of silicon nano-crystals

Nihed Chaâbane, Andriy V Kharchenko, Holger Vach and Pere Roca i Cabarrocas

Laboratoire de Physique des Interfaces et Couches Minces (UMR 7647 CNRS)
Ecole Polytechnique, 91128 Palaiseau Cedex, France
E-mail: chaabane@poly.polytechnique.fr

New Journal of Physics **5** (2003) 37.1–37.15 (http://www.njp.org/)
Received 5 February 2003
Published 28 April 2003

Abstract. We use silane-hydrogen plasmas to synthesize silicon nano-crystals in the gas phase and thermophoresis to collect them onto a cooled substrate. To distinguish between nano-crystals formed in the plasma and those grown on the substrate, as a result of surface and subsurface reactions, we have simultaneously deposited films on a conventional substrate heated at 250 °C and on a second substrate cooled down to 90 °C. A series of samples deposited at various discharge pressures, in the range of 400 mTorr to 1.2 Torr, have been characterized by Raman spectroscopy and ellipsometry. At low pressure (400–500 mTorr), the films are amorphous on the cold substrate and micro-crystalline on the hot one. As pressure increases, gas phase reactions lead to the formation of nano-crystalline particles which are attracted by the cold substrate due to thermophoresis. Consequently, we obtain nano-crystalline silicon thin films on the cold substrate and amorphous thin films on the heated one in the pressure range of 600–900 mTorr. Moreover, the analysis of the Raman spectra of the samples obtained on the cold substrate shows broadening and a small spectral shift as pressure is increased, indicating a decrease in crystal size with pressure. Finally, for yet higher discharge pressures (above 900 mTorr), the high reaction rates favour the formation of amorphous clusters resulting in the deposition of amorphous silicon films on both substrates.

PII: S1367-2630(03)59248-5

Contents

1. Introduction

The study of atomic clusters has become a very active area of research over the last decade. The main reasons for such an intense interest can be summarized as follows: first, the fundamental importance of a better understanding of how material properties change with increasing particle size, especially for the transitions: molecule → cluster → bulk [1, 2]; second, drastic improvement of experimental techniques for the production and analysis of clusters, providing new data about their electronic, chemical and structural properties [3]–[5]; third, the crucial role of clusters in a number of industrial applications such as the development of new semiconducting magnetic devices [6, 7], and finally, the use of clusters as building blocks (superatoms) to synthesize new solid or surface materials. Among these studies, nano-sized Si clusters have received a great deal of attention because of their technological applications.

The rapid growth of electronics often plays a catalyzing role in activating science and technology. Among many elementary technologies, silicon devices and their large scale integration techniques have been the basis for the progress in electronics. In order to highly integrate functional devices, it is necessary to develop new approaches for the nano-processing of various materials. These material processing technologies require the generation and the control of plasmas as well as that of particle production. Unluckily, there is a considerable lack of accurate and quantitative information on nano-particle formation during plasma processing. Methods are therefore needed to favour the formation and deposition of nanometre-sized particles on semiconductor devices during fabrication. Among them, radio-frequency plasmas are widely used in the manufacture of large area electronic devices and have been shown to produce nanometre-sized crystalline silicon particles [8].

In this paper, we use thermophoresis to demonstrate that, indeed, nano-crystalline silicon particles are formed in the gas phase, as opposed to surface and subsurface reactions of silane radicals [9]. Moreover, we show that it is possible to control the size of the nano-crystals by adjusting the plasma conditions. The analysis of the films by Raman spectroscopy and spectroscopic ellipsometry allows us to identify the conditions under which size-selected silicon nano-crystals are produced.

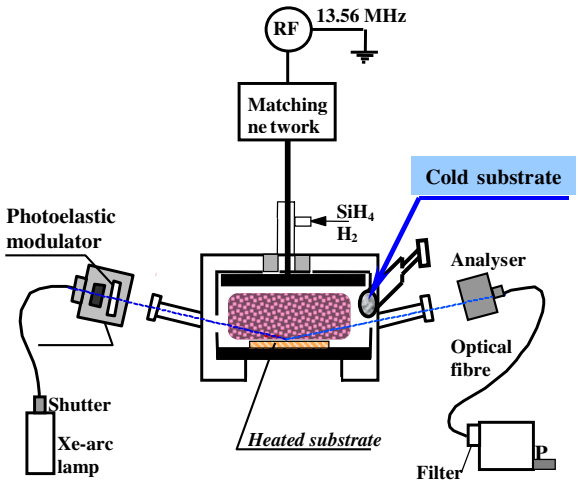

Figure 1. Schematic representation of the RFPECVD reactor.

2. Experiments

2.1. Film deposition

We use a standard capacitively coupled radio-frequency plasma enhanced chemical vapour deposition (RFPECVD) reactor to deposit silicon thin films. The general geometry, as shown in figure 1, consists of a cylindrical chamber with two parallel plate electrodes heated to 250 °C. The samples were deposited on Corning glass substrates from the dissociation of 10 sccm of silane diluted in 65 sccm of hydrogen under a RF power of 22 W for various gas pressures. Polymorphous silicon (pm-Si:H) thin films have been obtained using a wide range of plasma conditions, but which are always close to the formation of powder to allow the formation of Si clusters during the discharge [10]–[13].

In our previous studies, we have shown that the incorporation of silicon clusters and nano-crystals in the amorphous matrix leads to nano-structured films, which we have called pm-Si:H. These films clearly demonstrate improved transport properties and stability with respect to standard hydrogenated amorphous silicon (a-Si:H) [9]. However the concentration of nano-crystals in pm-Si:H films is very low (a few per cent) which makes their detection rather challenging. In order to enhance the incorporation of clusters and nano-crystals we used a new deposition strategy in which a water-cooled substrate holder is introduced in the reactor as shown in figure 1. The temperature of this substrate was measured to be 90 °C when the RF and standard substrate holder were heated to 250 °C. This arrangement of thermal boundary conditions results in a temperature gradient and thus a thermophoretic force on the particles which pushes them towards the cold substrate. Brock [14] carried out the first hydrodynamic analysis and found the following relationship for the thermophoretic force depending on the temperature gradient ∇T:

$$F_{th} = -6\pi^2 \mu \nu C_s (k_f/k_p + C_t Kn)[(1 + 3C_m Kn)(1 + 2k_f/k_p + 2C_t Kn)]^{-1} \nabla T/T$$

where C_s, C_t are, respectively, the thermal slip and temperature jump coefficients and C_m is the momentum exchange coefficient. k_p, k_f represent the thermal conductivity of the particle material and the fluid. Kn is the Knudsen number. μ and ν are, respectively, the absolute and

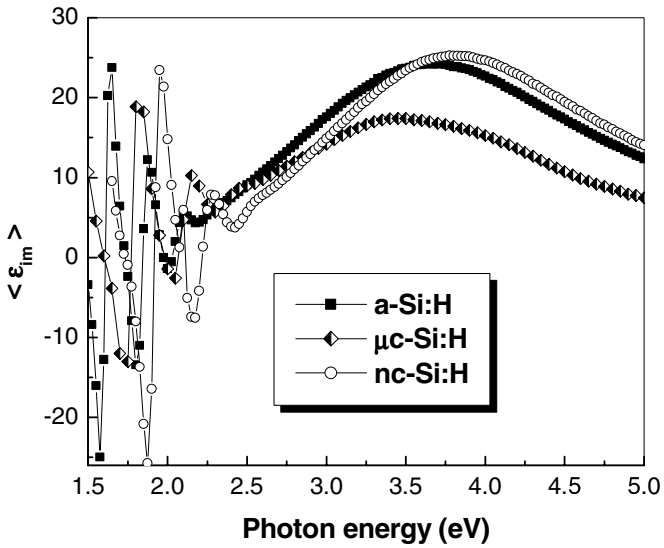

Figure 2. Examples of pseudo-dielectric function $\langle \varepsilon_{im} \rangle$ spectra for a-Si:H, μc-Si:H and nc-Si:H films.

kinematic viscosity. All these coefficients are obtained from the kinetic theory [15]. In the case of pm-Si:H deposition, we assume that the clusters are neutral because of their small size. Consequently, the two relevant forces acting on the particles that have to be considered are the viscous gas drag and the thermophoresis [16].

2.2. Raman spectroscopy

Raman spectroscopy is a very efficient technique for detecting the presence, and studying the structure, of silicon clusters in the deposited layers. Crystalline silicon is characterized by a strong and sharp TO band at 520 cm^{-1}. In the case of a-Si:H, the disorder induces changes in the vibrational density of states and its Raman spectrum is characterized by a large band at 480 cm^{-1} [17]. To calculate Raman shifts and peak broadening, the spectra are fitted as a sum of an amorphous and two crystalline contributions, assuming three Gaussians around 480, 520 and 507 cm^{-1}, respectively. The band at 507 cm^{-1} is associated with a bimodal distribution of grain sizes [18]. The Gaussian curve fitting method is applied to the Raman spectra after correction of the base line. The Raman spectra presented in this paper are the result of a scan with an irradiation duration of 300 s. We checked that the power of the He–Ne laser is small enough so that it cannot induce the crystallization of the sample.

2.3. Spectroscopic ellipsometry

Spectroscopic ellipsometry measurements were performed on samples simultaneously deposited on the hot (250 °C) and the cold (90 °C) substrate for various plasma pressures. Ellipsometry is a powerful technique for characterizing both thin films and interface micro-structures [19, 20]. The interpretation of ellipsometry data is dependent on the dielectric contrast between the different layers or the different constituent phases. Figure 2 shows spectral examples of the

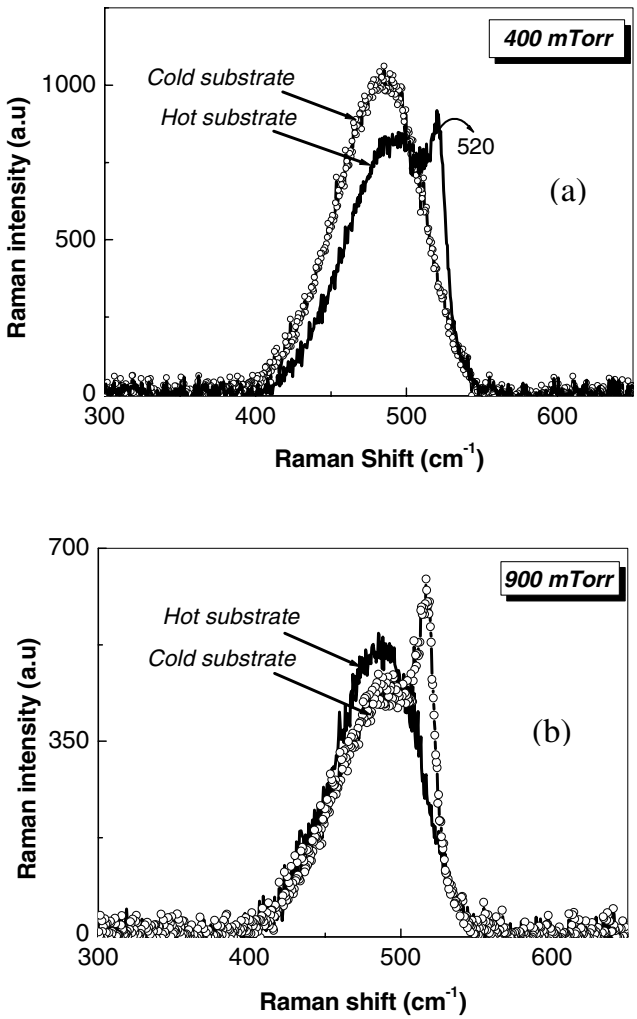

Figure 3. Raman spectra from Si layers deposited on cold and heated substrates at different pressures. (a) At 400 mTorr: a-Si:H on the cold substrate and μc-Si:H on the heated substrate and (b) at 900 mTorr: nc-Si:H thin films on the cold substrate and a-Si:H on the heated substrate.

pseudo-dielectric function for a-Si:H, nano-crystalline silicon (nc-Si:H) and micro-crystalline silicon (μc-Si:H) films deposited under our experimental conditions as described before. a-Si:H was deposited from the dissociation of pure silane at 40 mTorr pressure and a RF power of 5 W. The absorption spectrum of nano-crystalline silicon is slightly shifted towards higher energies compared to the amorphous material. The pseudo-dielectric functions of a-Si:H and nc-Si:H layers were modelled using the Tauc–Lorentz dispersion law [21] which gives information on the film thickness, its surface roughness and the Tauc–Lorentz parameters (E_g: band gap energy, A: broadening parameter, E_0: peak transition energy, C: relative disorder constant, ε_∞: real part of the dielectric function for higher energies). For the micro-crystalline material, the pseudo-dielectric function was modelled using the Bruggeman effective medium approximation (BEMA) [22].

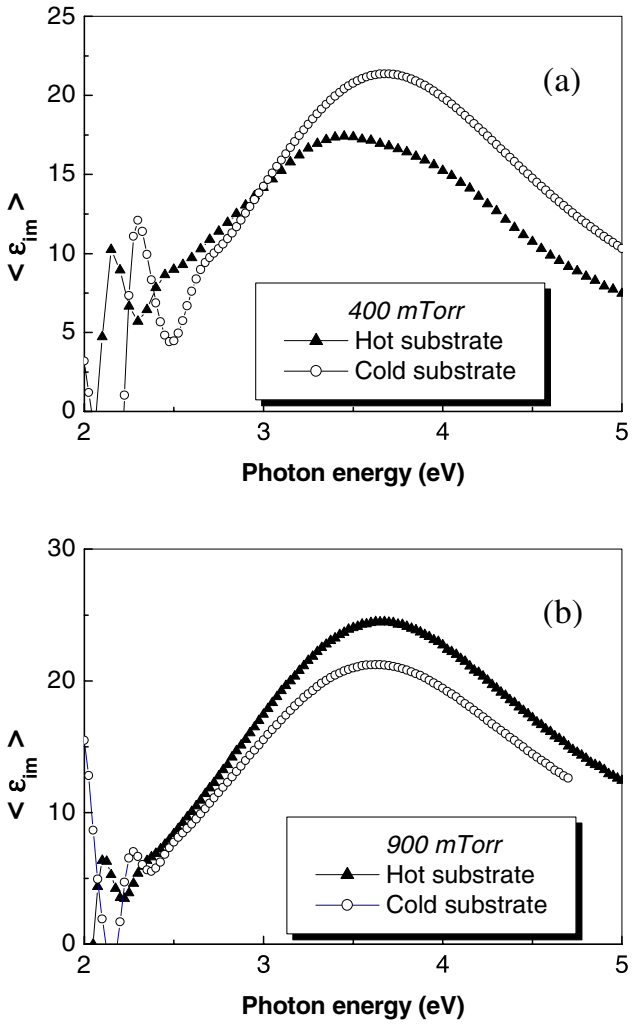

Figure 4. Imaginary part of the pseudo-dielectric function of hydrogenated silicon layers deposited on cold and heated substrates at the same conditions as in the last figure.

3. Results

Figure 3 shows the Raman spectra of thin films simultaneously deposited on the cold and the hot substrate at two different pressures. As shown in figure 3(a), the Raman spectra of films deposited at 400 mTorr shows a broad band for the sample deposited on the cold substrate, indicating that it is amorphous, while the sample deposited on the hot substrate presents a sharp peak at around 520 cm^{-1}, characteristic of the presence of crystallites. At 900 mTorr (figure 3(b)), we observe the opposite behaviour, i.e. the presence of a crystalline phase on the cold substrate, revealed by the appearance of a narrow Raman signal around 517 cm^{-1} that we attribute to the incorporation of nanometre sized particles in the deposited layers. This interpretation was previously suggested by Viera *et al* [23] and will be discussed in the following section. However, we observe standard a-Si:H on the heated substrate. These results clearly reveal the importance of the thermophoretic force on the structure of the films. They are supported by the results of our

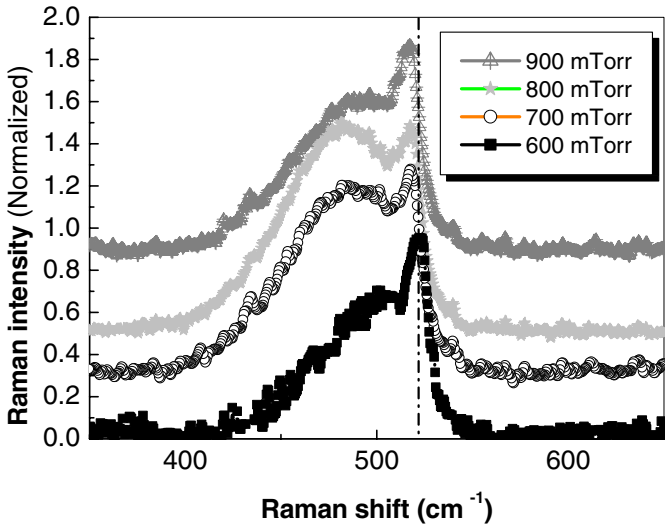

Figure 5. Effect of increasing pressure on nano-crystalline silicon (nc-Si:H) thin films deposited on the cold substrates (90 °C) using Raman spectroscopy.

Table 1. Results of the spectroscopic Raman measurements for samples of the cold and the conventional substrate. Values in parentheses correspond to peak positions and spectral widths as resulting from Gaussian fits.

Samples	Pressure (mTorr)	Hot substrate	Cold substrate
P12012	400	μc-Si:H	a-Si:H (480; 55) cm^{-1}
P12041	500	μc-Si:H	a-Si:H (481; 54) cm^{-1}
P12051	600	a-Si:H	μc-Si:H
P12052	700	a-Si:H	nc-Si:H
P12061	800	a-Si:H	nc-Si:H
P12062	900	a-Si:H	nc-Si:H
P12071	1000	a-Si:H	a-Si:H (478; 58) cm^{-1}
P12201	1200	a-Si:H	a-Si:H (478; 67) cm^{-1}

spectroscopic ellipsometry measurements. Indeed, as shown in figure 4, the imaginary part of the pseudo-dielectric function of the sample deposited at 400 mTorr on the hot substrate presents a shoulder at around 4 eV, characteristic of a micro-crystalline silicon film, while the sample deposited on the cold substrate has a broad peak centred at around 3.55 eV, characteristic of a-Si:H. At 900 mTorr, the spectrum obtained from the film deposited on the cold substrate shows a similar shape to the a-Si:H film obtained on the heated substrate, with a broad band centred at 3.55 eV.

Raman spectra of a series of samples deposited on the cold substrate at different pressures ranging from 600 to 900 mTorr are shown in figure 5. They indicate that the nc-Si:H thin films obtained by PECVD are a mixture of two phases, an amorphous matrix and ordered silicon domains or nano-crystallites. The position of these crystalline peaks are downshifted by approximately 3 cm^{-1} as compared to the TO peak position in crystalline silicon at 520 cm^{-1}, illustrated by the broken vertical line.

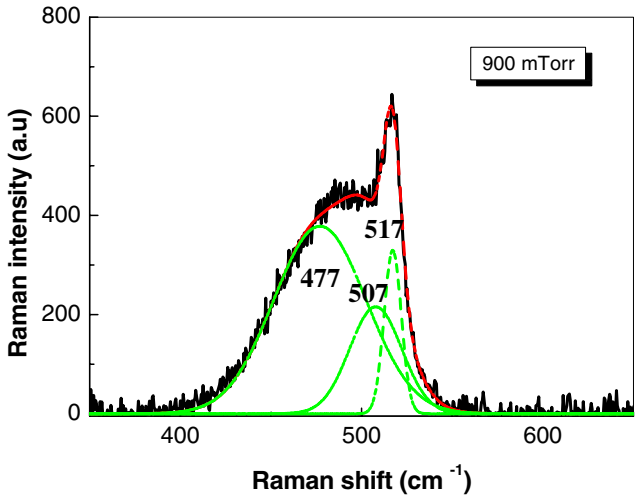

Figure 6. Raman spectrum decomposition into three Gaussian curves for a nano-crystalline Si film deposited at 900 mTorr on the cold substrate.

Table 1 summarizes the structure of the films co-deposited on the hot and cold substrates at various pressures. At 600 mTorr, we observe a transition from an amorphous to a nano-crystalline structure for samples deposited on the cold substrate, while we observe the opposite behaviour for samples deposited on the hot substrate. Moreover, for pressures above 900 mTorr, we observe a transition from nc-Si to a-Si:H on the cold substrate. Thus, nc-Si films are obtained on the cold substrate in the pressure range 600–900 mTorr. At pressures higher than 900 mTorr, the plasma conditions cause the material to grow as a-Si:H on both substrates as seen by our Raman measurements. However, at higher pressure silicon clusters can be incorporated into the films, leading to a particular structure (pm-Si:H) which has been studied in detail elsewhere [24].

In order to obtain quantitative information on the size and fraction of crystallites, we have analysed the Raman spectra in more detail. As an example, figure 6 shows the de-convolution of the Raman spectrum of a film deposited at 900 mTorr. The experimental spectrum can only be reproduced by the sum of three Gaussian peaks: the first one centred at 477 cm^{-1} corresponds to the a-Si:H matrix while the sharp peak at 517 cm^{-1} is related to the presence of nano-crystals. The remaining band at 507 cm^{-1}, often observed in nano- and micro-crystalline silicon films, has been attributed to the grain boundaries and/or to a distribution of grain sizes [17].

The same analysis was applied to the spectra presented in figure 5 and the results are summarized in table 2 where we present the position of each peak and its width at half maximum (FWHM). Moreover, we have also calculated the crystalline fraction F_c in each sample from the integrated intensities of the amorphous and crystalline peaks [22]. Table 2 shows that the crystalline fraction slightly increases with pressure, except for the sample deposited at 600 mTorr which has a crystalline fraction of 66%. Furthermore, the broadening of the crystalline peaks increases with pressure, suggesting that the size of the crystallites and their quality decrease with pressure. Finally for pressures above 1 Torr, no more crystallites are observed in the layer.

Ex situ spectroscopic ellipsometry measurements were performed in order to determine the thickness, surface roughness and composition of the films. The Tauc–Lorentz dispersion law was used to simulate the pseudo-dielectric function of amorphous and nano-crystalline materials [20]. This dispersion law describes the optical properties of a semiconductor in the

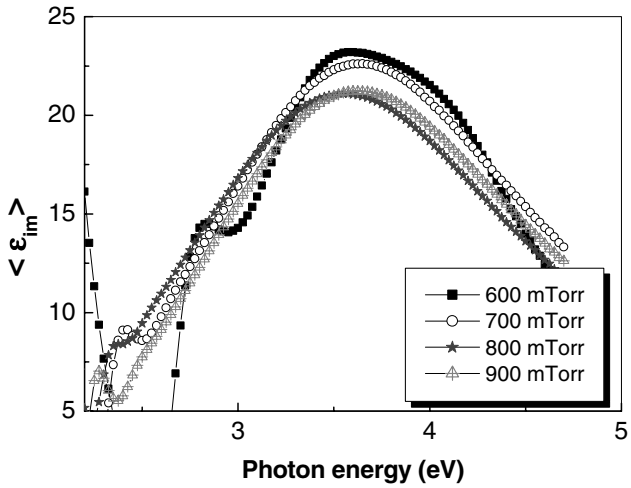

Figure 7. Imaginary part of the pseudo-dielectric function of nano-crystalline silicon (nc-Si:H) thin films deposited on cold substrates at different pressures.

Table 2. Evolution of the crystalline peak positions, their relative widths and the total crystalline fraction on the cold substrate as a function of gas pressure.

Pressure (mTorr)	Crystalline peak position (cm^{-1})	Width (cm^{-1})	Crystalline fraction (%) F_c
400		a-Si:H	
600	520 and 504	9.5 and 33	66
700	518 and 508	7.4 and 27	20
800	517 and 507	8.7 and 28	21
900	517 and 507	9.5 and 29	32
1000		a-Si:H	

spectral region above the gap. In figure 7, we plot the imaginary part of the measured pseudo-dielectric function of nano-crystalline films deposited at plasma pressures ranging from 600 to 900 mTorr, corresponding to table 2. The dielectric function of the various silicon films show a similar shape: a broad band centred between 3.5 and 3.75 eV. Note that the sample deposited at 600 mTorr shows a shoulder at about 4.2 eV which corresponds to a micro-crystalline material with a crystalline fraction of 71%, as deduced from BEMA analysis of the dielectric function, in good agreement with the Raman measurements (see table 2).

As shown in figure 8, a-Si:H material was obtained at 1 Torr on both the heated and the cold substrate. Even for the latter, no crystallites have been observed with Raman measurements (see figure 8(b)). Indeed, at 1 Torr particles formed in the gas phase agglomerate, resulting in the deposition of powders on the cold substrate as will be discussed in the following section. Consequently, the material appears to be amorphous. Especially for the cold substrate, however, the band is shifted by roughly 0.25 eV towards higher photon energies with respect to the sample deposited on the hot substrate (see figure 8(a)). This behaviour can be related to the incorporation of powders in the deposited layers as well as to the higher hydrogen content in the films deposited at 90 °C (cold substrate).

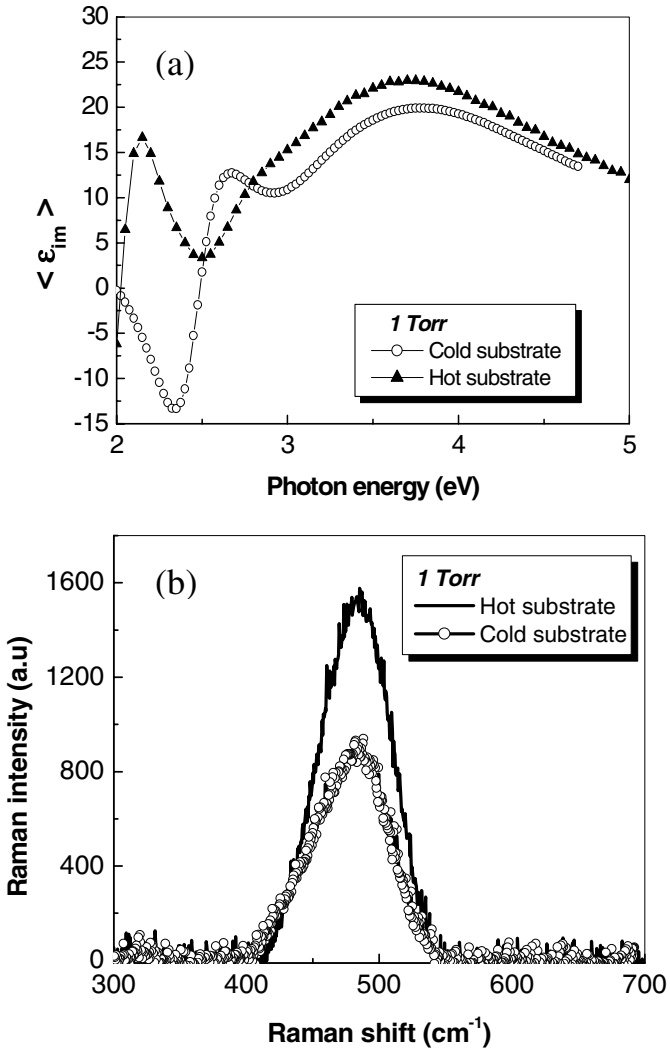

Figure 8. Imaginary part of the pseudo-dielectric function of different amorphous (a-Si:H) films deposited simultaneously on the cold and hot substrates at a plasma pressure of 1 Torr.

The results obtained from analysis of the pseudo-dielectric function using Tauc–Lorentz calculations [21] are summarized in table 3. Let us first focus on the surface roughness. As shown in the table, the incorporation of nano-crystals on the cold substrate samples is accompanied by a considerable increase in their surface roughness compared to that of the films co-deposited on the hot substrate. At 700 mTorr for example, the surface roughness increases from 4 Å on the hot substrate up to 37 Å on the cold one. As pressure increases the surface roughness on the cold substrate decreases, suggesting the incorporation of smaller crystallites during the growth, and becomes comparable to that of the heated substrate at 1000 mTorr. At this pressure, crystallites are no longer observed. At the same time, we observe that the gap energy E_g increases with pressure. It is also interesting to note that the parameter A (associated with the film density) monotonically increases in the pressure range of 700–900 mTorr and sharply decreases at 1000 mTorr, while the disorder parameter C strongly increases between 900 mTorr and 1 Torr.

Table 3. Results of the analysis of the ellipsometry spectra (Tauc–Lorentz parameters, layer roughness and thickness) obtained for samples simultaneously deposited on the cold (CS) and the hot substrate (HS). The same samples led to figures 5 and 6.

Samples	Substrate	Pressure (mTorr)	Thickness (Å)	Roughness (Å)	E_g (eV)	ε_∞	A	E_0 (eV)	C
P12051	CS	600			μc-Si:H ($F_c = 71\%$)				
	HS		3650	40	1.57	0.19	131	3.83	2.49
P12052	CS	700	2614	37	1.62	0.21	178	3.68	2.29
	HS		3037	4	1.58	0.23	188	3.57	2.34
P12061	CS	800	3877	35	1.64	0.31	184	3.77	2.31
	HS		4246	6	1.58	0.84	203	3.58	2.44
P12062	CS	900	3502	29	1.68	0.36	193	3.79	2.34
	HS		3796	6	1.57	1.04	195	3.67	2.45
P12071	CS	1000	887	3	1.83	1.14	179	3.66	2.43
	HS		1068	5	1.55	0.5	218	3.54	2.6

To demonstrate the presence of crystalline silicon domains in the amorphous matrix and to exclude any crystallization induced by the laser in the Raman measurements, ultra-thin silicon layers were deposited on copper micro-grids covered by a carbon layer to permit the use of high resolution transmission electron microscopy (HRTEM). Figure 9 shows a HRTEM image of the sample deposited at 900 mTorr under the same experimental conditions as the other samples characterized above by Raman spectroscopy and ellipsometry. The samples were examined with a Phillips CM3 HRTEM operating at 300 keV. In this image, we can see some crystallites of about 3 nm diameter embedded in a non-crystalline matrix.

4. Discussion

Spectroscopic ellipsometry and Raman are two powerful techniques for characterizing structural properties of films. In previous studies of pm-Si:H films in which nano-crystalline silicon particles are incorporated, Raman measurements hardly demonstrated the presence of the nano-crystals because of their smaller concentration in the layer [25]. Therefore, we have used thermophoresis in this study to increase the concentration of nano-crystals on the substrate and to give clear evidence of their formation in the gas phase. The effect of thermophoresis is demonstrated in figure 10, where we plot the Raman spectra for two samples successively deposited at 900 mTorr on the same substrate holder, but one with and the other without water cooling. The presence of the TO peak at 517 cm^{-1} when the substrate is cooled provides a clear demonstration of the presence of nano-crystals in the films as well as of the selective trapping of nano-crystals with respect to silicon radicals. In other words, we increase the ratio of nano-crystals with respect to silicon radical deposition on the cold substrate. Moreover, the fact that they are not present when the film is not cooled excludes any surface reaction which could induce crystallization through surface and subsurface reactions.

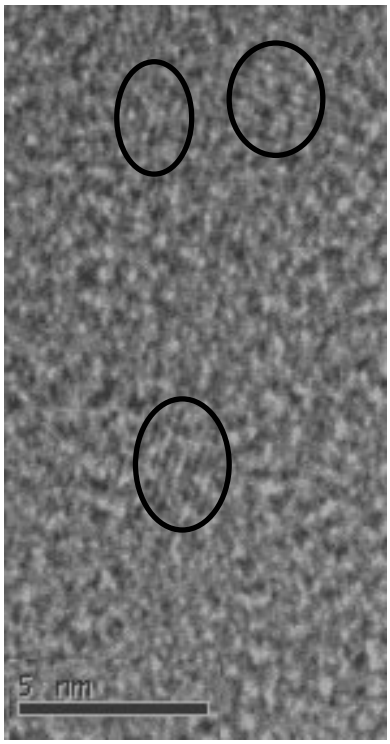

Figure 9. HRTEM image of a sample deposited at 900 mTorr on the cold substrate.

Combining the results shown in figures 3(a) and (b), corresponding respectively to (μc-Si:H and nc-Si:H deposition conditions, we confirm that micro-crystalline material growth at lower pressures is controlled by surface and bulk reactions of deposited radicals and atomic hydrogen [26]. Indeed, at 400 mTorr, corresponding to pristine plasma conditions, the crystalline peak was detected on the heated substrate, but not on the cold one. In contrast, at 900 mTorr, where gas phase reactions lead to the formation of clusters and nano-crystals, we observe a crystalline peak on the cooled substrate, but not on the heated one. Since the steps in a CVD process are sequential, the one that occurs at the lowest rate will determine the overall deposition rate. These CVD steps can be grouped into gas phase and surface processes. Gas phase processes dictate the rate at which radicals impinge on the surface and are proportional to the gas diffusion and the concentration gradient. Moreover, the surface reaction rate is greatly affected by the surface temperature. At low temperatures, the surface reaction rate is reduced so much that the arrival rate of reactants can exceed the rate at which they are consumed by surface reaction processes. Consequently, we obtained amorphous material on the cold substrate for lower pressures (see figure 3(a)). At higher pressures, in contrast, we obtained nano-crystalline layers since nano-particles are formed in the gas phase (see figure 3(b)). These crystallites were observed in nc-Si:H films deposited in the pressure range from 700 to 900 mTorr (see table 1). Raman spectra of these nano-crystalline films deposited on the cold substrate are plotted in figure 5 to illustrate the shift of the crystalline peaks with pressure. The detailed analysis of these spectra shows a broadening and small additional spectral shifts suggesting, respectively, a more disordered material and a decrease in crystal size with increasing pressure (see table 2). The spectroscopic ellipsometry data of these pressure series show the same tendencies. In fact, ellipsometry analysis of the

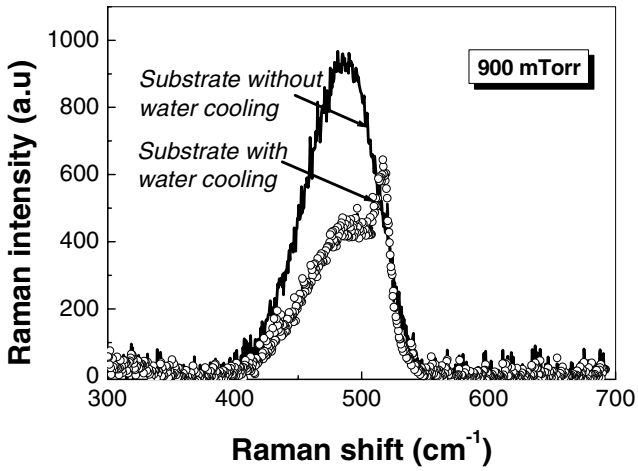

Figure 10. Raman spectra of two thin films successively deposited at 900 mTorr on the same substrate. The symbol curve corresponds to the Raman spectrum resulting from the deposition on the water cooled substrate (90 °C). The black curve results from exactly the same deposition conditions, but without any water cooling, i.e. from a substrate temperature of 180 °C.

films deposited at 400 mTorr indicates the deposition of micro-crystalline material on the heated substrate and amorphous material on the cold one (see figure 4(a)). At 600 mTorr, we obtained μc-Si:H material on the cold substrate as deduced from Raman and ellipsometry measurements (see figures 5 and 7), but we must note the presence of the second crystalline peak at 504 cm^{-1}, indicating the presence of nano-crystalline particles. In the case of films deposited at 700 and 800 mTorr the crystalline fraction is roughly 20% (see table 2). The ellipsometry spectra of the samples deposited on the cold substrates at pressures ranging from 700 to 900 mTorr (see figure 7) have the same shape as a-Si:H film displayed in figure 2 with a shift by about 0.25 eV to higher energies.

The slight increase in optical band gap E_g with pressure for samples deposited on cold substrates, as shown in table 3, can be related to an increase in the hydrogen content of the films or to a decrease in crystalline cluster size [27]–[29], which is in agreement with our previous observations obtained from the Raman spectra analysis where a broadening and small spectral shifts towards lower energies were observed (see table 2). Interestingly, the Tauc–Lorentz disorder parameter C is found to increase with pressure, corresponding to a more disordered material. In other words, as pressure increases, the deposited nano-crystalline material becomes more and more disordered which agrees remarkably well with the broadening of the Raman crystalline peak. This observation suggests that the size of the incorporated crystallites decreases with plasma pressure between 700 and 900 mTorr, i.e. the smallest crystallites are obtained at 900 mTorr. Using equation (1), we can deduce the crystallite size from the measured Raman shift [22]:

$$\Delta\omega(D) = -A(a/D)^{\gamma} \tag{1}$$

where $\Delta\omega(D)$ is the Raman shift induced by the presence of nano-crystals with a diameter D, taking as reference the position of the micro-crystalline peak at 520 cm^{-1}, $a = 0.543$ nm is the network constant of Si, A = 47.41 cm^{-1} and $\gamma = 1.44$ are fitting parameters that describe

the phonon confinement in nanometric spheres of diameter D. As shown in figure 6, the first Raman peak position, characterizing the most important crystalline fraction, is around 517 cm^{-1}. Consequently, the size of crystalline particles that are formed in the gas phase and that become trapped on the cold substrate is about 3.5 nm, corresponding to a shift $\Delta\omega$ of about 3 cm^{-1}. This calculated nano-particle size is in good agreement with the particle size measured by HRTEM as shown in figure 9.

Moreover, the nano-particle size decreases in the pressure range of 600–900 mTorr as previously discussed. Accordingly, the film roughness slightly decreases as demonstrated in table 3, which seems to be linked to the decrease in nano-crystal size. At pressures above 900 mTorr, the plasma regime changes, favouring the formation of powders in the gas phase. Thus, a critical cluster or nano-particle concentration is reached favouring their coagulation, i.e. the particles react with each other resulting in a sharp decrease of particle concentration in the gas phase. Since the deposition rate increases with pressure, the particles formed do not have time to arrange themselves to obtain a minimum energy structure before their deposition leading to amorphous material.

For each pressure, it is also interesting to note that the decrease in A and increase of E_0 for samples deposited simultaneously on cold and hot substrates could be related to a higher void fraction and a higher hydrogen content, suggesting the incorporation of hydrogenated nano-particles in the deposited layers on the cold substrate. Moreover, the higher order observed in films deposited at lower pressures is due to the low void fraction resulting in a more dense material as previously shown in figure 7. Indeed, the $\langle \varepsilon_{im} \rangle$ amplitude is the highest for the densest sample.

All samples deposited on the cold substrate show a relatively dense material. Roughly the same pseudo-dielectric function amplitudes are obtained as for amorphous material deposited on the heated substrate (see figure 2). Therefore, in obtaining such dense material let us suppose the possibility of an ion contribution to the deposited layers that can form the amorphous phase between the deposited nano-crystallites.

5. Conclusion

We have used thermophoresis to demonstrate the formation of silicon nano-crystals in the plasma and to trap them on a cooled substrate. Comparing the properties of films deposited on heated and cooled samples under various pressures which cover the range from a pristine to a dusty plasma, we have been able to control the size of nano-particles. The highest investigated discharge pressures favour the formation of amorphous clusters and powders resulting in the deposition of a-Si:H films. While much more studies are required to fully characterize the structure of the nano-crystals, in particular their hydrogen related structure, the present results will already help us to better control the deposition of nano-crystalline silicon films.

Acknowledgment

This work has been partially financed by the French 'Ministère de la Recherche' through the 'ACI Nanostructures programme'.

References

[1] Corcoran E 1990 *Sci. Am.* **263** 122
[2] Bjornholm S 1990 *Contemp. Phys.* **31** 309
[3] Elkind J L, Alford J M, Weiss F D, Laaksonen R T and Smalley R E 1987 *J. Chem. Phys.* **87** 2397
[4] Anderson L R, Maruyama S and Smalley R E 1991 *Chem. Phys. Lett.* **176** 348
[5] Maus M, Ganteför G and Eberhardt W 2000 *Appl. Phys.* A **70** 535
[6] Guskos N, Likodemos V, Patapis S K, Typek J, Wabia M, Fuks H, Gamari-seale H, Walczak J, Himmel I R and Rosacka M 1997 *J. Solid State Chem.* **137** 223
[7] Léon M C, Coronado E, Mascaros J R, Gomez C J, Kovira C and Lauhkin V N 2000 *Synth. Met.* **103** 2339
[8] Viera G, Mikikian M, Bertran E, Roca i Cabarrocas P and Boufendi L 2002 *J. Appl. Phys.* **92** 4684
[9] Roca i Cabarrocas P 2000 *J. Non-Cryst. Solids* **266–269** 31
[10] Roca i Cabarrocas P, Gay P and Hadjadj A 1996 *J. Vac. Sci. Technol.* A **14** 655
[11] Roca i Cabarrocas P, Hamma S, Sharma S N, Viera G, Bertran E and Costa J 1998 *J. Non-Cryst. Sol.* **227** 871
[12] Boufendi L, Plain A, Blondeau J Ph, Bouchoule A, Laure C and Toogood M 1992 *Appl. Phys. Lett.* **60** 169
[13] Bertran E, Sharma S N, Viera G, Costa J, Stahel P and Roca i Cabarrocas P 1998 *J. Mater. Res.* **13** 2476
[14] Brock J R 1962 *J. Colloid Sci.* **17** 768
[15] Batchelor G K and Shen C 1985 *J. Colloid Interface Sci.* **107** 1
[16] Foncuberta i Morral A and Roca i Cabarrocas P 2001 *Thin Solid Films* **383** 161
[17] Rinnert H, Vergnat M and Burneau A 2001 *J. Appl. Phys.* **89** 237
[18] Touir H, Dixmier J, Zellama K, Morhange J F and Alkaim P 1998 *J. Non-Cryst. Solids,* **227–30** 906
[19] Aspnes D E, Theeten J B and Hottier F 1979 *Phys. Rev.* B **20** 3292
[20] Feng G F, Katiyar M, Abelson J R and Maley N 1992 *Phys. Rev.* B **45** 9013
[21] Jellison G E and Modine F A Jr 1996 *Appl. Phys. Lett.* **69** 371
[22] Bruggeman D A G 1935 *Ann. Phys., Lpz.* **24** 636
[23] Viera G, Huet S and Boufendi L 2001 *J. Appl. Phys.* **90** 4175
[24] Roca i Cabarrocas P, Fontcuberta i Morral A, Lebib S and Poissant Y 2002 *Pure Appl. Chem.* **74** 359
[25] Butté R 2000 *Thesis* Université Claude Bernard
[26] Roca i Cabarrocas P, Hamma S, Hadjadj A, Bertomeu J and Andreu J 1996 *Appl. Phys. Lett.* **69** 529
[27] Pederson M R, Porezag D V, Hujnal Z and Fruenheim Tk 1996 *Phys. Rev.* B **54** 2863
[28] Santos P V, Koopmans B, Esser N, Schmidth W G and Bechstedt F 1996 *Phys. Rev. Lett.* **77** 759
[29] Katirciogla S and Erkoc S 2001 *Physica* E **9** 314